1   **Auxin is not asymmetrically distributed in initiating Arabidopsis leaves**

2   **Neha Bhatia[1] and Marcus G. Heisler[1*]**

3

4   **Affiliations**

5   [1]School of Life and Environmental Sciences, University of Sydney, NSW, Australia

6   *Author for correspondence: Marcus G Heisler (marcus.heisler@sydney.edu.au)

7   **Abstract**

8   It has been proposed that asymmetric auxin levels within initiating leaves help

9   establish leaf polarity, based in part on observations of the DII auxin sensor. Here we

10   show that the mDII control sensor also exhibits an asymmetry and that according to

11   the ratio-metric auxin sensor R2D2, no obvious asymmetry in auxin exists. Together

12   with other recent findings, our results argue against the importance of auxin

13   asymmetry in establishing leaf polarity.

14

15   **Introduction**

16   The leaves of seed plants are usually flat with distinct cell types making up their

17   dorsal (upper) and ventral (lower) tissues. A fundamental question in plant development

18   is how this dorsal-ventral polarity is first specified. Studies based on wounding

19   experiments have suggested the presence of an inductive signal originating from the

20   meristem that promotes dorsal identity in the adaxial (adjacent to the meristem) tissues

21   of the leaf primordium[1,2]. However more recently, it was found that exogenous

22   application of the plant hormone auxin to tomato leaf primordia resulted in the

23   formation of radialized leaves that appeared ventrilized. Hence, relatively high levels

24   of auxin are proposed to promote ventral or inhibit dorsal leaf cell fate[3]. Extending

25   these conclusions, it was also proposed that an asymmetry in the auxin distribution

26   across the leaf adaxial-abaxial axis at leaf initiation acts to help specify leaf polarity

27   during regular development[3]. A critical piece of evidence supporting this latter proposal

28   is that an auxin sensor, the DII[4,5] indicates low levels of auxin in adaxial leaf tissues

29   compared to abaxial tissues at leaf initiation[3]. Hence asymmetries in auxin

30   concentrations between the adaxial and abaxial leaf tissues, as a result of PIN1 mediated

31   auxin transport, are proposed to help establish leaf polarity[3]. Building on this

32   conclusion, a more recent study proposed that low levels of auxin in adaxial tissues are

33   necessary to restrict the expression of the WOX1 and PRS genes to the middle domain,

34   since auxin promotes their expression[6]. Finally, the reported asymmetry in auxin has

35   also been linked to asymmetries in the mechanical properties of leaf tissues and their

36   morphogenesis[7].

37

38   Despite these studies, reason to reassess the role of any asymmetry in auxin in

39   specifying leaf polarity has arisen due to the recent finding that the expression patterns

40   of genes involved in leaf dorsoventrality are already patterned in meristem tissues

41   where leaves originate, with little change occurring to their expression during organ

42   initiation. Hence leaf polarity appears pre-patterned [8]. Furthermore, rather than

43   compromise dorsal cell fate, auxin was found to promote dorsal cell fate by maintaining

44   Class III HD-ZIP expression and repressing KAN1 expression in the adaxial cells of

45   organ primordia[8], which is the opposite of what would be expected according to the

46   auxin asymmetry hypothesis. In addition, Caggiano et al. (2017) also found that

47   exogenous auxin application to young leaf primordia did not influence the spatial

48   pattern of WOX1 and PRS, only the intensity of expression[8]. This also conflicts with

49   the proposal that low levels of auxin are required in adaxial leaf tissues to prevent

50   ectopic WOX1 and PRS expression as previously proposed[6].

51

52   **Results and discussion**

53   Given the concerns listed above, we decided to examine the distribution of auxin during

54   leaf initiation using not only by the DII sensor assessed in previous studies but also, by

55   looking more closely at the expression pattern of the non-auxin degradable mDII auxin

56   sensor control[4] as well as the ratiometric R2D2 auxin sensor[9]. We initially focused on

57   the first two leaves three and four days after stratification (DAS), when these leaves are

58   initiating as well as a day later as they begin to elongate and included the PIN1-GFP

59   marker in our analysis to correlate auxin levels with PIN1 expression and polarity. At

60   3DAS, the expression patterns of REV and KAN1 are already polar within such

61   primordia, although the FIL expression domain at this stage of development is still

62   being refined[8]. Also at this stage, PIN1 is polarized towards the distal tip of leaf

63   primordia but has reversed polarity away from the primordia, towards the meristem, in

64   cells adjacent to the primordia on the adaxial side. According to the ratio-metric auxin

65   sensor R2D2, auxin concentrations were relatively low in adaxial cells of the primordia

66   but also low in abaxial and lateral regions proximally (Fig1-a and d). High levels of

2

67   auxin were only found in more distal regions towards the tip of the primordia, matching
68   the overall pattern of signal from PIN1-GFP. No obvious asymmetry in signal between
69   the adaxial and abaxial sides of the primordia was observed. This same overall pattern
70   of signal was found in 16 out of 18 leaves that were examined. At 4DAS, the auxin
71   distribution according to the R2D2 sensor was more uniform although higher levels of
72   auxin appeared associated with the vasculature, again correlating with PIN1 expression
73   (n=12/12 leaves) (Fig. 1 g and j).

74

75   As our results using the R2D2 auxin sensor indicate a different auxin distribution
76   compared to that reported previously using the DII marker [3], we next re-examined the
77   pattern of DII auxin sensor expression at the same developmental stages. In contrast to
78   the R2D2 pattern, the DII pattern showed an asymmetry of expression in leaf primordia
79   at 3 DAS, indicating relatively low auxin levels in adaxial primordium cells, as found
80   previously. DII signal appeared strongest in the adaxial epidermis but was also stronger
81   in the adaxial sub-epidermal cell layer compared to abaxial epidermal and sub-
82   epidermal cell layers (Fig.1- b, e and h) (n=18/18 leaves). One day later, although DII
83   signal was still higher in the adaxial cells of the primordia, it started to show a relatively
84   increased expression in the abaxial sub-epidermal layers as well compared to earlier
85   stage (n=13/14 leaves) (Fig1-k). Overall our results using the DII marker are similar to
86   those obtained previously and consistent with the proposal that there are low levels of
87   auxin in the adaxial regions of leaf primordia, in contrast to our results using the R2D2
88   sensor. Given this discrepancy, we next examined the expression of the mDII sensor
89   which is driven by the same 35S promoter as the DII sensor but is not auxin sensitive.
90   Surprisingly we found that, like the DII results, expression of the mDII marker was also
91   higher in the adaxial cells of the primordia (n= 16/16 leaves) (Fig.1-c,f and i). The
92   pattern appeared almost identical to the pattern found using the DII marker except that
93   the mDII marker also showed high levels of expression in the shoot meristem whereas
94   the DII sensor did not (compare Fig1-b and c). The similarity of expression between
95   DII and mDII was also apparent at 4DAS when the leaves had started to elongate (Fig.1-
96   l) (n=14/14 leaves). To verify the auxin sensitivity of the sensors used we imaged
97   seedlings before and after treatment with 5mM NAA and found a strong decrease in
98   DII expression compared to mDII and an increase in the ratio of VENUS compared to
99   tdTomato signal for the R2D2 sensor, consistent with an increase in auxin levels (Figure
100   S1).

101

102   All together these results indicate that the asymmetry in expression found previously

103   for the DII auxin sensor in very young leaf primordia[3] is not due to an asymmetry in

104   auxin levels but rather, likely due to differences in transcription driven by the 35S

105   promoter used to drive both DII and mDII in adaxial compared to abaxial leaf tissues.

106   We note that although a single section showing control expression of mDII in older

107   leaves was cited by Guan et al., (2017)[10], our results show that this information was not

108   adequate for assessing similarities and differences between DII and mDII at early

109   developmental stages. To check whether adaxial expression in leaf primordia is a

110   characteristic common to other reporters driven by the 35S promoter, we also examined

111   the expression of 35S::H2B-mRFP1 and 35S::EGFP-LTI6b which had previously been

112   combined into the same plant line by crossing[11]. Surprisingly the expression patterns

113   for these markers were not only different to the mDII marker but also different to each

114   other with the H2B marker showing stronger expression in the adaxial and abaxial

115   epidermis and the LTI6b marker showing a more uniform pattern (Fig. S2). These

116   results reveal that even when the same promoter is utilized to drive FP (fluorescent

117   protein) expression, distinct differences in intensity patterns can occur *in planta*. This

118   may be due to differences in the position of T-DNA insertion in the genome or

119   differences in the surrounding DNA of the vector used. All together then, our results

120   highlight the importance of using ratio-metric sensors for *in vivo* measurements since

121   otherwise it is difficult to adequately control for differences in signal intensity due to

122   promoter activity or other confounding factors. Finally, while the R2D2 marker utilizes

123   a single transgene to express two distinct FPs from two identical promoters[9], a

124   potentially improved approach to assess auxin levels *in vivo* may be to utilize a single

125   promoter to drive the auxin-dependent degradation domain II from Aux/IAA proteins

126   linked to a tandem fusion of fast and slowly folding FP variants, such as VENUS and

127   mCherry. Such an approach can enable a more direct readout of protein degradation

128   rates[12,13] and therefore potentially improve measurements of relative auxin

129   concentration.

130

131   While our findings are inconsistent with the proposal that asymmetries in the auxin

132   distribution influence leaf polarity[3], pattern WOX/PRS gene expression [6] or regulate

133   tissue mechanics[7], they also leave other observations unexplained. In particular, to

134   understand the apparent ventrilization of leaf primordia in tomato in response to

4

135   exogenous auxin[3] will require further work in assessing how auxin distribution patterns

136   change in response to exogenous treatments and how auxin is distributed during regular

137   development in tomato, preferentially using a ratio-metric auxin sensor such as R2D2.

138

139   **Methods**

140   **Plant material and growth conditions.**

141   Seeds of the plants expressing *p35S::DII-VENUS* and *p35S::mDII-VENUS* transgenes

142   (*Columbia* ecotype) were obtained from Dr. Teva Vernoux [4]. R2D2 reporter line

143   carrying *pPIN1::PIN1GFP* transgene (*Landsberg* ecotype) has been described

144   previously[9,14]. Seeds were germinated and grown on GM medium (pH-7 with 1M

145   KOH) containing 1% sucrose, 1X Murashige and Skoog salts (Sigma M5524), MES 2-

146   (MN-morpholino)- ethane sulfonic acid (Sigma M2933), 0.8 % Bacto Agar (Difco),

147   1% MS vitamins (Sigma M3900) in long day conditions.

148

149   **Confocal imaging and data analysis**

150   Seedlings aged 3DAS (days after stratification) and 4DAS were dissected as described

151   previously[14]. Dissected seedlings were then oriented appropriately to obtain a view of

152   the young leaves either from above or from the side. Seedlings were imaged live, on a

153   Leica TCS-SP5 upright confocal laser scanning microscope with hybrid detectors

154   (HyDs) using a 25X water objective (N.A 0.95). VENUS was imaged using argon laser

155   (excitation wavelength 514nm) while tdTomato was imaged using a white light laser

156   (excitation wavelength 561 nm). Z-stacks were acquired in a 512x512 pixel format with

157   section spacing of 1μm and line averaging 2.

158

159   Ratio-metric calculations for R2D2 auxin sensor were performed using ImageJ (FIJI,

160   https://fiji.sc) as described previously[14]. All the images were processed using IMARIS

161   9.0.0 (bit-plane). Optical sections (transverse or longitudinal) were reconstructed using

162   orthogonal slicer in IMARIS.

163

164   **Auxin treatment**

165   Seedlings aged 3DAS were dissected imaged and treated with approximately 10μL of

166   5mM NAA (1-Napthaleneacetic acid) solution in water (0.5M stock in 1M KOH) for

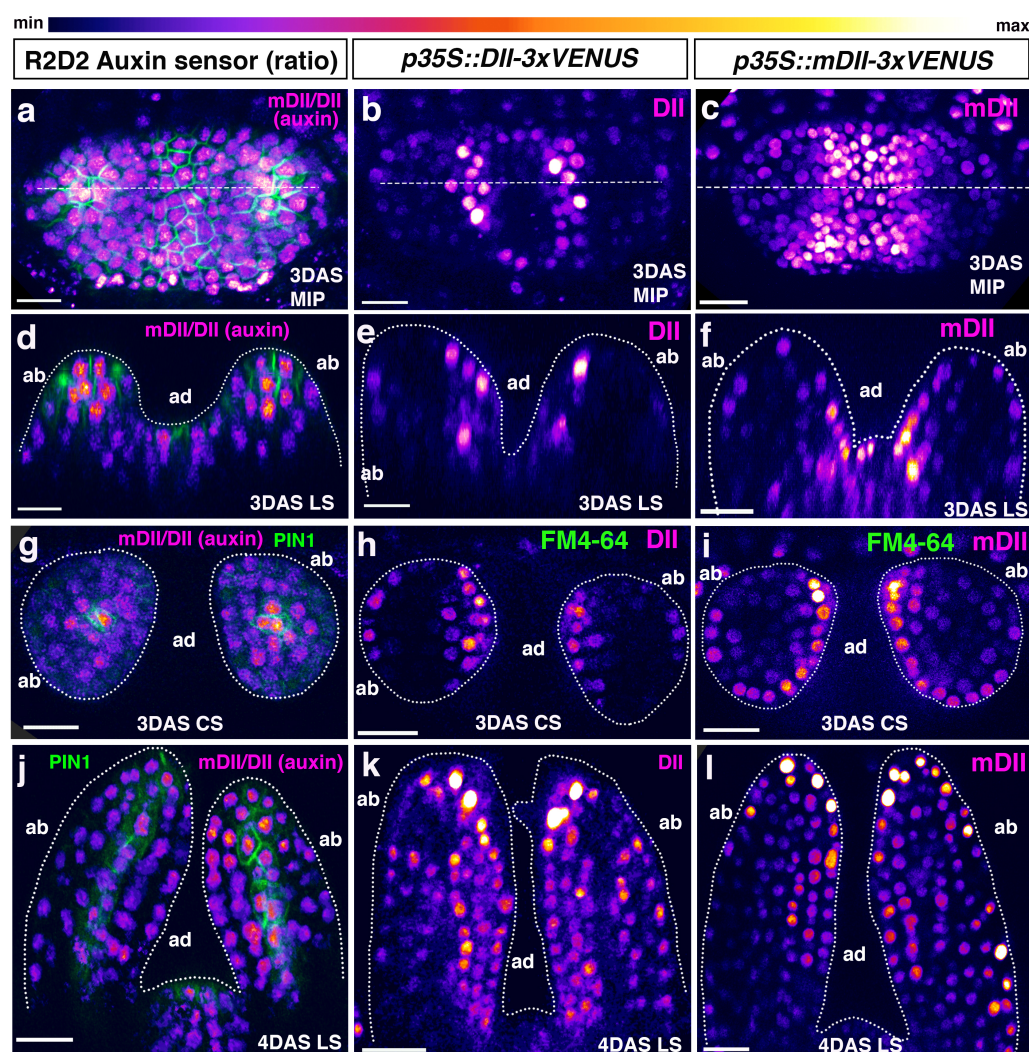167   60 minutes and imaged again with same settings as prior to treatment.

168

Acknowledgements

175

References

1   Sussex, I. M. Morphogenesis in Solanum tuberosum I: experimental investigation of leaf dorsiventrality and orientation in the juvenile shoot. *Phytomorphology* **5**, 286-300 (1955).

2   Reinhardt, D., Frenz, M., Mandel, T. & Kuhlemeier, C. Microsurgical and laser ablation analysis of leaf positioning and dorsoventral patterning in tomato. *Development* **132**, 15-26 (2005).

3   Qi, J. *et al.* Auxin depletion from leaf primordia contributes to organ patterning. *Proc Natl Acad Sci U S A* **111**, 18769-18774, doi:10.1073/pnas.1421878112 (2014).

4   Brunoud, G. *et al.* A novel sensor to map auxin response and distribution at high spatio-temporal resolution. *Nature* **482**, 103-106, doi:10.1038/nature10791 (2012).

5   Vernoux, T. *et al.* The auxin signalling network translates dynamic input into robust patterning at the shoot apex. *Mol Syst Biol* **7**, 508, doi:10.1038/msb.2011.39 (2011).

6   Guan, C. *et al.* Spatial Auxin Signaling Controls Leaf Flattening in Arabidopsis. *Curr Biol* **27**, 2940-2950 e2944, doi:10.1016/j.cub.2017.08.042 (2017).

7   Qi, J. *et al.* Mechanical regulation of organ asymmetry in leaves. *Nat Plants* **3**, 724-733, doi:10.1038/s41477-017-0008-6 (2017).

8   Caggiano, M. P. *et al.* Cell type boundaries organize plant development. *eLife* **6**, doi:10.7554/eLife.27421 (2017).

9   Liao, C. Y. *et al.* Reporters for sensitive and quantitative measurement of auxin response. *Nat Methods* **12**, 207-210, 202 p following 210, doi:10.1038/nmeth.3279 (2015).

10   Wang, Y. *et al.* The Stem Cell Niche in Leaf Axils Is Established by Auxin and Cytokinin in Arabidopsis. *Plant Cell* **26**, 2055-2067, doi:10.1105/tpc.114.123083 (2014).

11   Federici, F., Dupuy, L., Laplaze, L., Heisler, M. & Haseloff, J. Integrated genetic and computation methods for in planta cytometry. *Nature Methods* **9**, 483-U104, doi:10.1038/nmeth.1940 (2012).

12   Khmelinskii, A. *et al.* Tandem fluorescent protein timers for in vivo analysis of protein dynamics. *Nat Biotechnol* **30**, 708-714, doi:10.1038/nbt.2281 (2012).

13   Barry, J. D., Dona, E., Gilmour, D. & Huber, W. TimerQuant: a modelling approach to tandem fluorescent timer design and data interpretation for

213   measuring protein turnover in embryos. *Development* **143**, 174-179,
214   doi:10.1242/dev.125971 (2016).
215 14 Bhatia, N. *et al.* Auxin Acts through MONOPTEROS to Regulate Plant Cell
216   Polarity and Pattern Phyllotaxis. *Curr Biol* **26**, 3202-3208,
217   doi:10.1016/j.cub.2016.09.044 (2016).
218
219
220
221
222

Figure 1 Predicted auxin distribution in young leaves as indicated by different auxin sensors.

(a-c) Confocal projections of *Arabidopsis* seedlings aged 3DAS (days after stratification) showing predicted auxin distribution based on the ratio-metric auxin sensor R2D2 (magenta) along with PIN1-GFP (green) (a); expression pattern of *p35S::DII-VENUS* (magenta) (b) and *p35S::mutatedDII-VENUS* (mDII, magenta) (c).

(d-f) Longitudinal reconstructed optical sections of (a-c), respectively, along the dashed lines. **(g-i)** Representative examples of transverse reconstructed optical sections of 3DAS Arabidopsis seedlings showing predicted auxin distribution as indicated by the R2D2 sensor along with PIN1-GFP expression (g), DII-VENUS expression (h) and mDII-VENUS expression (i). R2D2 auxin sensor indicates low but symmetric auxin levels on adaxial and abaxial sides and relatively high auxin levels at the distal tip and in the provasculature where PIN1 expression is also high (d, g). DII-VENUS is more strongly expressed adaxially indicating low auxin levels on the adaxial side of the

238   leaves relative to the abaxial side. However, mDII-VENUS also shows high expression

239   on the adaxial side of the leaf (compare e, h with f, i) and in the shoot meristem. **(j-l)**

240   Representative examples of longitudinal reconstructed optical sections of 4DAS

241   Arabidopsis seedlings showing predicted auxin distribution by R2D2 sensor along with

242   PIN1-GFP expression (green) (i), DII-VENUS expression (j) and mDII-VENUS

243   expression (k). At this stage, the R2D2 sensor indicates a more uniform auxin

244   distribution in the leaf but higher auxin levels in the vasculature where PIN1-GFP

245   expression is also high (j). DII-VENUS shows slightly high expression in adaxial cells

246   and an absence of expression in the vasculature (k). mDII-VENUS shows a similar

247   pattern to DII but is also expressed in the vasculature (l). Scale bars 15μm (a-i) and
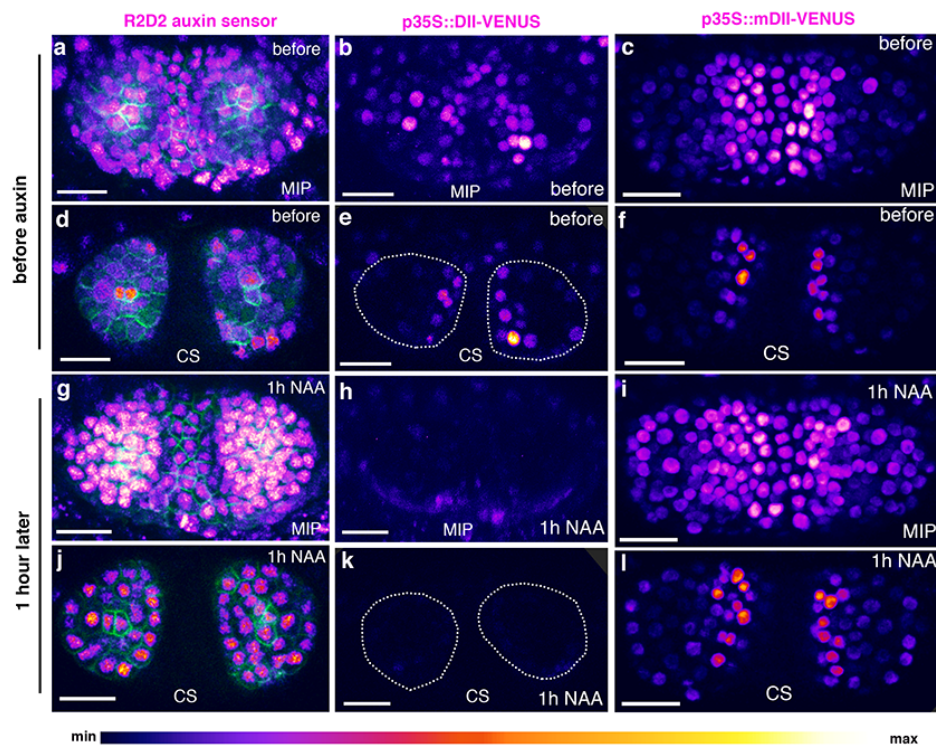
248   20μm (j-l).

249

Figure S1 Response of different auxin sensors to external auxin application

(a-f) Confocal projections (a-c) and transverse optical reconstructions (d-f) of *Arabidopsis* seedlings, 3DAS, showing predicted auxin distribution based on R2D2 ratio-metric sensor (magenta) along with PIN1-GFP expression in green (a,d), DII-VENUS sensor (magenta) (b,e) and mDII-VENUS sensor (magenta) (c, f) before auxin application. **(g-l)** Confocal projections (g-i) and transverse optical reconstructions (j-l) of *Arabidopsis* seedlings, 3DAS, showing predicted auxin distribution based on R2D2 ratio-metric sensor (magenta) along with PIN1-GFP expression in green (a,d), DII-VENUS sensor (magenta) (b,e) and mDII-VENUS sensor (magenta) (c, f) 1hour after the application of 5mM NAA. Note, R2D2 sensor indicates an increased and broadening of auxin levels after NAA application (compare d and j) (n=3/3). Consistently, DII-VENUS shows an attenuated expression within 1 hour of auxin application (compare b,e with h,j) (n=4/4). mDII-VENUS levels do not decrease upon auxin application (compare c,f with i,l) (n=4/4). Scale bars 20μm (a-l).
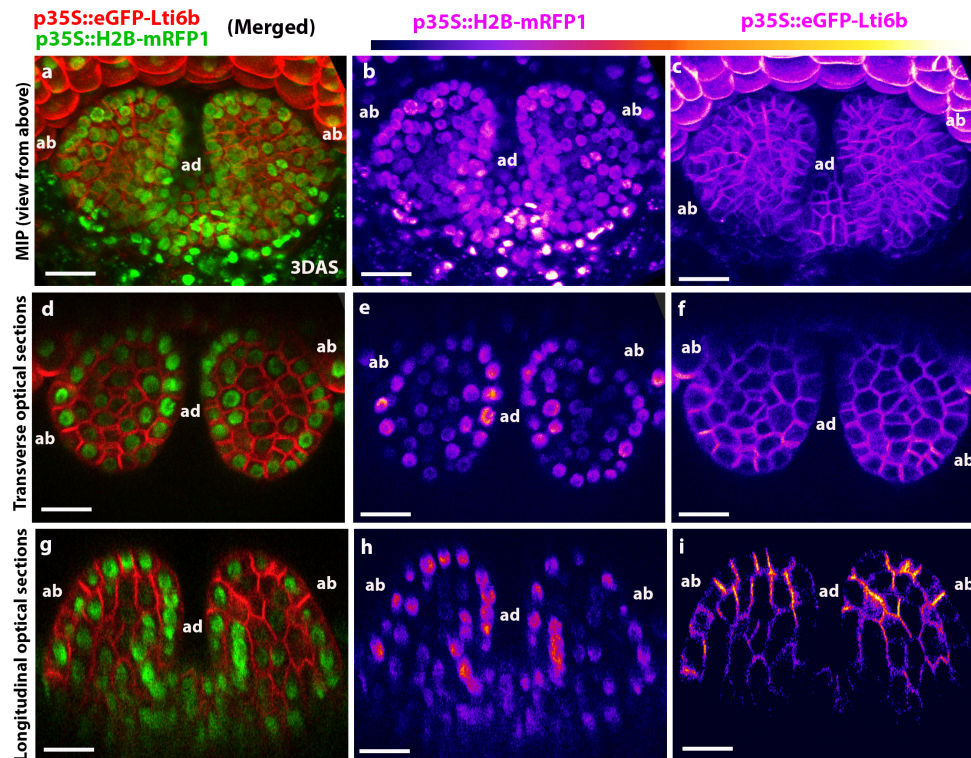
10

267 Figure S2

268

269

270

271 **Figure S2**

272

273 **Different 35S promoter-driven reporter genes show different expression patterns**

274 **in young leaves.**

275

276 **(a-c)** Confocal projections of *Arabidopsis* seedlings aged 3DAS showing expression

277 patterns of a *p35S:eGFP-Lti6b* (membrane marker, green) and *p35S::H2B-*

278 *mRFP1*(nuclear marker red) together (a), *p35S::H2B-mRFP1* only (magenta) (b) and

279 *p35S:eGFP-Lti6b* only (magenta) (c). **(d-f)** Transverse optical reconstructions of (a-c)

280 respectively; merged (d), *p35S::H2B-mRFP1* only (magenta) (e) and *p35S:eGFP-Lti6b*

281 only (magenta) (f). **(g-i)** Longitudinal optical reconstruction of (a-c) respectively;

282 merged (g), *p35S::H2B-mRFP1* only (magenta) (h) and *p35S:eGFP-Lti6b* only

283 (magenta) (i). Note *p35S::H2B-mRFP1* shows similarly high levels of expression in

284 both adaxial (ad) as well as abaxial (ab) epidermal cell layers and weaker expression in

285 the middle regions (e and h). However, *p35S:eGFP-Lti6b* shows no consistent

11

286   asymmetry in expression throughout the leaf (f and i). Scale bars 20μm (a-i), (n=10

287   leaves).

288